



## Ferromagnetism and microstructure in Cr implanted p-type (100) silicon

L.J. Gao<sup>a,b,\*</sup>, L. Chow<sup>c</sup>, R. Vanfleet<sup>d</sup>, K. Jin<sup>a,b</sup>, Z.H. Zhang<sup>a,b</sup>, X.F. Duan<sup>a,b</sup>, B. Xu<sup>a,b</sup>, B.Y. Zhu<sup>a,b</sup>, L.X. Cao<sup>a,b</sup>, X.G. Qiu<sup>a,b</sup>, B.R. Zhao<sup>a,b</sup>

<sup>a</sup> National Laboratory for Superconductivity, Institute of Physics, Chinese Academy of Sciences, Beijing 100190, China

<sup>b</sup> Beijing National Laboratory for Condensed Matter Physics, Chinese Academy of Sciences, Beijing 100190, China

<sup>c</sup> Department of Physics, University of Central Florida, Orlando, FL 32816, USA

<sup>d</sup> Department of Physics, Brigham Young University, Provo, UT 84604, USA

### ARTICLE INFO

#### Article history:

Received 7 May 2008

Received in revised form

16 July 2008

Accepted 24 July 2008 by X.C. Shen

Available online 30 July 2008

#### PACS:

61.72.Vv

75.50.Pp

75.50.Dd

#### Keywords:

A. Cr

B. Ion implantation

B. Anneal

D. Ferromagnetism

### ABSTRACT

The magnetic properties and microstructure of p-type Si (100) implanted with  $1.0 \times 10^{15} \text{ cm}^{-2}$  of Cr ions at 200 keV have been investigated by a superconducting quantum interference device (SQUID) magnetometer, scanning electron microscope (SEM) and transmission electron microscopy (TEM). The magnetic hysteresis loops and saturation magnetization of 0.67–0.75 emu/g in a wide temperature range are observed in the as-implanted sample. Annealing of the as-implanted sample modifies the microstructure and therefore weakens the magnetic exchange interaction. TEM observations show that the as-implanted silicon layer is amorphous. After annealing at temperature  $\geq 800 \text{ }^\circ\text{C}$ , the SEM showed that the implanted profile layer became blurred and narrow, the ferromagnetism was weakened, which should have resulted from the re-crystallization of the implanted amorphous layer. These results were further compared with magnetic hysteresis observed in Mn-implanted silicon.

© 2008 Elsevier Ltd. All rights reserved.

## 1. Introduction

Transition metal impurities are fast diffusers in silicon [1]. Even at low concentration, it still can negatively impact the reliability and performance of silicon based semiconductor devices [2]. For this reason, the study of the distribution and diffusion of transition metal ions in silicon has been an important subject. Previously, one of the authors studied the diffusion profiles of high dosage chromium implanted into silicon [3]. It was found that the chromium profiles after thermal annealing at different temperatures were strongly influenced by the microstructures of the implanted silicon.

Recently, Bolduc et al. [4] have demonstrated that Mn ions implanted silicon showed unexpected room temperature ferromagnetism. This finding has stimulated many new investigations on the magnetic behavior of Mn ions implanted silicon [5–10], Mn ions implanted germanium [11,12], and Mn ions implanted into

compound semiconductors, such as GaAs [13], GaN [14], GaP [15], and  $\text{TiO}_2$  [16]. The main interest in the Mn ion-implanted semiconductors materials is related to the search for room temperature dilute magnetic semiconductors for future spintronics device applications [4].

By comparison, the investigations of ferromagnetism due to other 3d transition metals in semiconductors are relatively rare. Osterwalder et al. [17] investigated Cr doped  $\text{TiO}_2$  films grown by molecular beam epitaxy technique. They found in-plane ferromagnetic order in the anatase phase  $\text{TiO}_2$  but not in the rutile phase. Singh et al. [18], on the other hand, investigated Cr doped GaN thin films grown by reactive molecular beam epitaxy. They found that Cr in GaN can have high fraction of substitutional sites. Their results demonstrated that the location of the Cr sites in GaN lattice plays an important role in determination of its magnetic properties. Misiuk et al. [19] investigated on the effects of various temperatures and different pressure treatment of Cr implanted silicon on its diffusion, structural and optical properties. In addition, they found that ferromagnetism appears at 5 K on Cr implanted sample annealed at  $450 \text{ }^\circ\text{C}$  and 1.1 GPa high pressure. Li et al. [20] observed ferromagnetism for Cr ions implanted ZnO thin films at room temperature.

In the present study, we investigate Cr-ion implantation in p-type (100) silicon. The implanted profile of these samples has been

\* Corresponding author at: National Laboratory for Superconductivity, Institute of Physics, Chinese Academy of Sciences, Beijing 100190, China. Tel.: +86 10 82649182; fax: +86 10 82649193.

E-mail address: [gaolijuanlinda@gmail.com](mailto:gaolijuanlinda@gmail.com) (L.J. Gao).

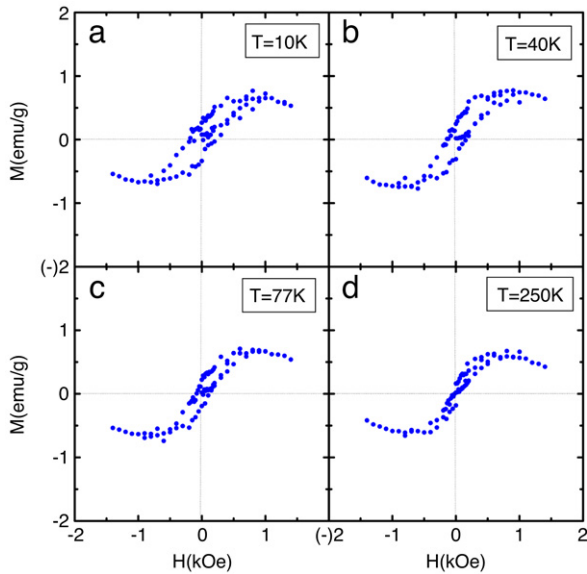


**Fig. 1.** Magnetization versus magnetic field  $M$ - $H$  curves for Cr-ion implanted p-type (100) silicon at various temperatures. (a) at 10 K (b) at 40 K (c) at 77 K (d) at 250 K.

investigated in detail for the implanted profile by means of secondary ion mass spectroscopy (SIMS) [3,21]. Here we focused our effort on the investigation of the magnetic property of this system and the relationship between magnetism and microstructures. We have observed the formation of ferromagnetism in the as-implanted sample through the magnetization versus temperature ( $M$ - $T$ ) behavior and magnetization versus magnetic field ( $M$ - $H$ ) hysteresis loops measurements. The structural feature associated with ion implantation and annealing process is also obtained by scanning electron microscopy (SEM) and transmission electron microscopy (TEM) analyses.

## 2. Experimental

Cr ions were implanted into p-type (100) single crystal silicon substrates with a dosage of  $1.0 \times 10^{15}$  ions- $\text{cm}^{-2}$  and implantation energy of 200 keV at room temperature. Implantation was carried out at Implant Science Corporation.

To investigate the formation of ferromagnetism, the magnetization versus magnetic field ( $M$ - $H$ ) hysteresis loops and magnetization versus temperature ( $M$ - $T$ ) measurements were performed using a superconducting quantum interference device (SQUID) magnetometer (Quantum Design MPMS-5). In order to understand the annealing effect on Cr-ions implantation, thermal annealing was carried out for the as-implanted sample after magnetization

measurement at temperature 800 °C for 5 min in Ar (99.99%) of 50 Pa, then magnetism measurements were performed again.

At the same time, in order to examine the structure modification due to Cr-ion implantation and annealing process, the SEM and TEM are used to observe the cross sectional profile of the implanted layer before and after thermal annealing.

## 3. Results and discussion

Fig. 1 shows the magnetization versus magnetic field relation of the as-implanted sample in temperatures of 10 K, 40 K, 77 K, and 250 K. From the distinguished ferromagnetic hysteresis loops of the as-implanted sample at each temperature, the saturation magnetization values of 0.67–0.75 emu/g at these temperatures is obtained. This is estimated from the implanted depth of  $\sim 250$  nm determined by SEM profile depth (Fig. 2(a)). It is shown that with decreasing temperature the ferromagnetism is enhanced, similar to the behavior of the bulk ferromagnetic materials. It should be noted that for as-implanted case, the saturation magnetization value of Cr-ions implanted silicon is larger than that of Mn-ions implanted silicon [4]. This may be caused by different distribution of implanted Cr-ions and Mn-ions in silicon. This also may indicate that Cr-Si system is more suitable to form dilute magnetic semiconductor. At the same time, it is found that the coercive field of the implanted Cr-Si system ranges from 88 Oe at 250 K to 210 Oe at 10 K as shown in Fig. 3. From the temperature dependence of coercive field (Fig. 3) and the temperature dependence of the saturation magnetization (Fig. 1), the Curie temperature of ferromagnetic exchange interaction associated with the implanted Cr ions (moments) is estimated to be at least  $>250$  K, indicating a strong long-range ferromagnetic ordering. Fig. 4 shows the magnetization versus temperature ( $M$ - $T$ ) curves for the same sample as above, which is obtained by zero field cooling and measured at field of 0.1 T. The line (a) corresponds to magnetization before annealing and the line (b) corresponds to that after annealing at 800 °C for 5 min. It is obvious that the magnetization  $M(T)$  is decreased when annealing treatment is carried out, consistent qualitatively with the results of  $M(H) \sim T$  relation (Fig. 1). When the annealing temperature is increased to 800 °C and above, the hysteresis loop is weakened dramatically (not show here).

These measured data correspond well to SEM examinations. It can be seen that the SEM image (Fig. 2(a)) obtained before annealing shows a quite clear bright (white) Cr-ion implanted region, the depth can be defined as  $\sim 250$  nm. After annealing, the Cr-ion implanted profile examined by SEM becomes blurred and the implanted area becomes narrow (Fig. 2(b)). To obtain further understanding about this, cross sectional TEM measurement is used to examine the Cr-ions implanted layer. It is observed that the implanted layer shows amorphous morphology (Fig. 5(a)).

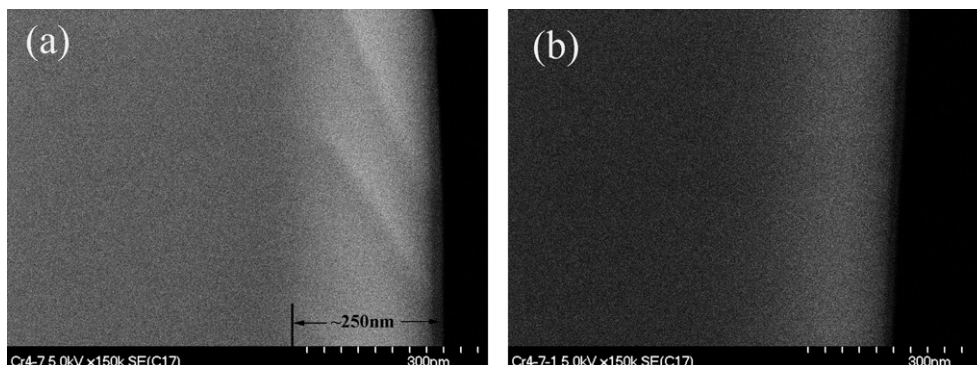


**Fig. 2.** SEM image of Cr-ion implanted p-type (100) silicon (a) before annealing (b) after annealing.

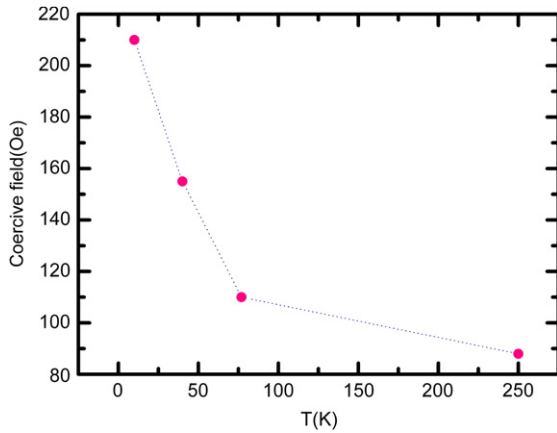


Fig. 3. Coercive fields at various temperatures for Cr-ion implanted p-type (100) silicon.

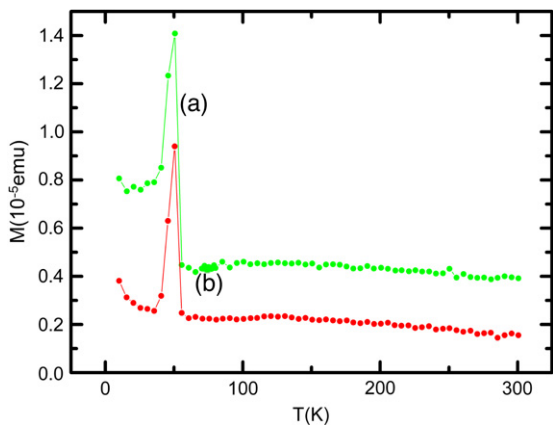


Fig. 4. Magnetization versus temperature  $M$ - $T$  curves for Cr-ion implanted p-type (100) silicon. By ZFC and measured at 0.1 T. (a) before annealing (b) after annealing, the peak at  $\sim 50$  K is caused by oxygen, not from the sample.

This is reasonable, because in the present work, the dosage is  $1 \times 10^{15} \text{ cm}^{-2}$ , which is well above the amorphization threshold dosage of  $1 \times 10^{14} \text{ cm}^{-2}$  [22]. It is further clearly indicated that between the implanted layer and unimplanted silicon crystal, there is a transition region where crystallization silicon and amorphous silicon coexist as shown in Fig. 5(b), this implanted amorphous area should be entirely recovered to crystallized silicon, since the higher temperature annealing is actually a recrystallization process [22]. Therefore, the change of SEM image after annealing implies that the amorphous layer caused by the

implantation (dosage of  $1.0 \times 10^{15} \text{ cm}^{-2}$  and energy of 200 keV) is gradually recrystallized and the implanted Cr ions tend to pile up at the surface, when the annealing temperature is increased to  $800^\circ\text{C}$ . The SIMS depth profile shows a corresponding situation when temperature is increased to  $800^\circ\text{C}$  and above [5]. All these should reasonably correspond to the weakening of the magnetization after higher temperature annealing.

To further understand the formation process of Cr-Si dilute magnetic semiconductor, the intrinsic origin of ferromagnetism should be considered. It is well known that Cr metal is an antiferromagnet at low temperature, it also shows spin density wave (SDW) in nature. The ion implantation should lead to two aspects of changes: (1) the ion-implanted layer tends to be amorphous silicon when the dosage is larger enough, then the interaction of irradiation induced defects and Cr-ions may be an important factor to promote the formation of ferromagnetism. In our case, the ferromagnetism forms in as Cr-ion implanted silicon and sharply weakens after annealing at temperature  $\geq 800^\circ\text{C}$ , very possibly indicating the evidence of interaction of implanted Cr ions and defects for ferromagnetism; (2) by ion implantation, even short-range ordering antiferromagnetic exchange coupling of Cr-ions tend to be broken down, and the Cr-ion spins tends to exchange couple to be long-rang ordered ferromagnet. It should be stressed that for the present ion-implanted case, the long-range ordering ferromagnetism is believed to be intrinsic in nature within the whole implanted layer, then the long-range ordering ferromagnetism should be indeed to be formed based on dilute magnetic moments, in this case, the medium for exchange coupling is needed, i.e., the holes acting as the medium are very possible in such p-type silicon matrix [4–6]. Another argument that the ferromagnetism is attributed to magnetic nanoparticles was proposed for Mn-ion implanted silicon [8], but such kinds of nanoparticles are not found in our Cr-ion implanted silicon samples by TEM and SEM observations. On the other hand, it can be considered that the annealing treatment will also lead to two changes: (1) The amorphous silicon tends to be recrystallized, when the annealed temperature is high enough ( $>500^\circ\text{C}$ ) [3]. (2) The implanted Cr-ions tend to be piled up to the surface of the silicon substrate and escape from the surface of it when annealing temperature is increased further, resulting in weakening the ferromagnetic ordering. It may also be considered that the piled up high density Cr-ions during higher temperature annealing may have a tendency of recovering of antiferromagnetic exchange interaction again (i.e., tending to be bulk-like Cr) and leads frustration for formation of ferromagnet. At the same time, it has been found that the escape of Cr-ions from silicon at annealing temperature  $\geq 800^\circ\text{C}$  happens more easily than other transition metals [21]. All of the above should be the reason that the annealing at temperature  $\geq 800^\circ\text{C}$ , leads the ferromagnetic

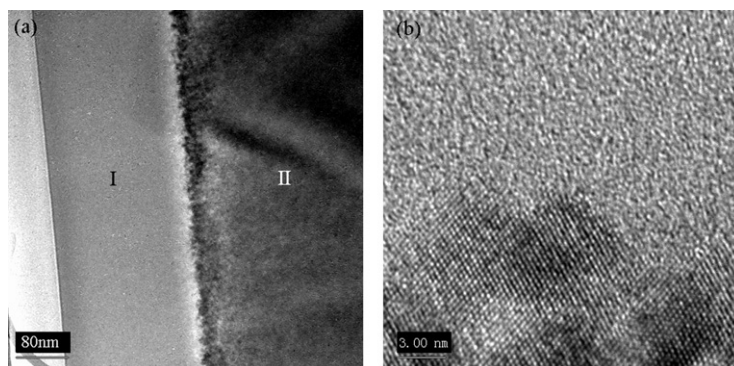


Fig. 5. TEM images of Cr-ion implanted p-type (100) silicon (a) image of morphology of implanted layer: I implanted amorphous area, II unimplanted silicon crystal area; (b) high resolution image of the transition area between implanted layer and unimplanted crystal silicon body within which both amorphous and crystalline parts can be seen clearly.

magnetization to be remarkably weakened in our Cr-ion implanted case, this contrasts sharply with the annealing result of Mn-ion implantation [5].

#### 4. Conclusion

The Cr-ion implantation in p-type (100) silicon is carried out, and SEM, TEM and SIMS consistently display the implantation process and effects, especially, the formation of dilute magnetic semiconductor in the Cr-ion implanted amorphous layer is realized, i.e., quite strong long-range ordering ferromagnetism is successfully obtained in as implanted samples in a wide temperature range. But the annealing process leads the Cr-ion implanted amorphous silicon layer to be recrystallized, resulting in weakening and disappearing of ferromagnetism. Such Cr-ion implantation in silicon provides an effective route to realize the formation of a dilute magnetic semiconductor, for which the mechanism must be investigated further.

#### Acknowledgments

L.J. Gao and B.R. Zhao thank W.W. Huang et al. for their measurement support. This work is supported by Grants from the State Key Program for Basic Research of China and the National Natural Science Foundation. L. Chow acknowledges financial support from Apollo Technologies, Inc. and the Florida High Tech Corridor Research Program.

#### References

- [1] E.R. Weber, *Appl. Phys. A* 30 (1983) 1.
- [2] K. Graff, *Metal Impurities in Silicon-device Fabrication*, 2nd ed., Springer, Berlin, 2001.
- [3] P. Zhang, F. Stevie, R. Vanfleet, R. Neelakantan, M. Klimov, D. Zhou, L. Chow, *J. Appl. Phys.* 96 (2004) 1053.
- [4] M. Bolduc, C. Awo-Affouda, A. Stollenwerk, M.B. Huang, F.G. Ramos, G. Agnello, V.P. LaBella, *Phys. Rev. B* 71 (2005) 033302.
- [5] M. Bolduc, C. Awo-Affouda, F. Ramos, V.P. LaBella, *J. Vac. Sci. Technol. A* 24 (2006) 1648–1651.
- [6] A.B. Granovskii, Yu.P. Sukhorukov, A.F. Orlov, N.S. Perov, A.V. Korolev, E.A. Gan'shina, V.I. Zinenko, Yu.A. Agafonov, V.V. Saraikin, A.V. Telegin, D.G. Yarkin, *J. Exp. Theor. Phys. Lett.* 85 (2007) 335–338.
- [7] A. Wolska, K. Lawniczak-Jablonska, M. Klepka, M.S. Walczak, A. Misiuk, *Phys. Rev. B* 75 (2007) 113201.
- [8] S. Zhou, K. Potzger, G. Zhang, A. Mücklich, F. Eichhorn, N. Schell, R. Grötzschel, B. Schmidt, W. Skorupa, M. Helm, J. Fassbender, *Phys. Rev. B* 75 (2007) 085203.
- [9] S. Ma, Y. Sun, B. Zhao, P. Tung, X. Zhu, W. Song, *Solid State Commun.* 140 (2006) 192.
- [10] L. Zeng, E. Helgren, M. Rahimi, F. Hellman, R. Islam, B.J. Wilkens, R.J. Culbertson, D.J. Smith, *Phys. Rev. B* 77 (2008) 073306.
- [11] S. Picozzi, L. Ottaviano, M. Passacantando, G. Profeta, A. Continenza, F. Priolo, M. Kim, A.F. Freeman, *Appl. Phys. Lett.* 86 (2005) 062501.
- [12] A. Verna, et al., *Phys. Rev. B* 74 (2006) 085204.
- [13] N.A. Sobolev, M.A. Oliveira, V.S. Amaral, A. Neves, et al., *Mater. Sci. Eng., B* 126 (2006) 148–150.
- [14] N. Theodoropoulou, A.F. Hebard, M.E. Overberg, C.R. Abernathy, S.J. Pearton, S.N.G. Chu, R.G. Wilson, *Appl. Phys. Lett.* 78 (2001) 3475.
- [15] N. Theodoropoulou, A.F. Hebard, S.N.G. Chu, M.E. Overberg, C.R. Abernathy, S.J. Pearton, R.G. Wilson, J.M. Zavada, *J. Appl. Phys.* 91 (2002) 7499.
- [16] F. Iacomi, N. Apetroaei, G. Calin, et al., *Thin Solid Films* 515 (2007) 6402.
- [17] J. Osterwalder, T. Droubay, T. Kaspar, J. Williams, C.M. Wang, S.A. Chambers, *Thin Solid Films* 484 (2005) 289–298.
- [18] R.K. Singh, S.Y. Wu, H.X. Liu, L. Gu, *Appl. Phys. Lett.* 86 (2005) 012504.
- [19] A. Misiuk, A. Barcz, L. Chow, B. Surma, J. Bak-Misiuk, M. Prujarczyk, *Solid State Phenomena* 131–133 (2008) 375–380.
- [20] H. Li, J.P. Sang, F. Mei, F. Ren, L. Zhang, C. Liu, *Appl. Surf. Sci.* 253 (2007) 8524.
- [21] F. Salman, P. Zhang, L. Chow, F.A. Stevie, *Mater. Sci. Semicond. Process.* 9 (2006) 62.
- [22] K.S. Jones, S. Prussin, E.R. Weber, *Appl. Phys. A* 45 (1988) 1.